European Society of Computational Methods in Sciences and Engineering (ESCMSE)

Journal of Numerical Analysis, Industrial and Applied Mathematics (JNAIAM)
vol. 5, no. 3-4, 2011, pp. 141-152
ISSN 1790–8140

Landmark-Based Registration Using a Local Radial Basis Function Transformation[1]

R. Cavoretto[2], A. De Rossi[3]

Department of Mathematics,
University of Turin,
via C. Alberto 10,
I–10123, Turin, Italy

B. Quatember[4]

Innsbruck Medical University (Radiology),
Anichstrasse 35,
6020 Innsbruck, Austria

Received 19 January, 2009; accepted in revised form 18 December, 2010

Abstract: In this paper we propose the use of a local image transformation involving radial basis functions for landmark-based registration of medical images. More precisely, we consider radial basis functions as nodal functions in the modified Shepard method. In this way we obtain an image transformation more accurate and stable than the one given by the global radial basis functions, as shown by numerical results.

Keywords: thin plate spline, scattered data interpolation, elastic registration, medical imaging, local algorithms.

Mathematics Subject Classification: 68U10, 65D05.

PACS: 02.60.Gf, 02.60.Ed.

1 Introduction

The problem of image registration consists in finding a transformation which gives accurate matching of two or more images. In general, one of the images is viewed as a *source* image and the other one as a deformable *target* image.

In applications a transformation function $\mathbf{h} : \mathbb{R}^d \to \mathbb{R}^d$, where d is the image dimension, e.g. $d = 2, 3$, for $2D$ and $3D$ images, respectively, is reached. The basic idea is to determine the transformation such that each landmark of the source image is mapped onto the corresponding

[1]Published electronically December 30, 2010
[2]E-mail: roberto.cavoretto@unito.it
[3]Corresponding author. E-mail: alessandra.derossi@unito.it
[4]E-mail: Bernhard.Quatember@uibk.ac.at

landmark of the target image (see [15, 17, 18, 20, 21]). This problem can be formulated in the context of multidimensional interpolation on scattered data, and solved using the *radial basis function* (RBF) method (see [7, 11, 23] for an exhaustive presentation of the method). Among the several proposed methods, RBF is the most suitable when the number of points to be interpolated is small (as is typically the case with manually placed landmarks). The use of RBF transformations for point–based image registration, and in particular of the thin plate spline (TPS), was first proposed by Bookstein [6], and it is still common (see the recent paper [19] and the software package MIPAV [16]). The thin plate spline yields minimal bending energy properties, so that the result is an overall smooth deformation. On the other hand, RBFs have a global support when used to obtain a global transformation. Therefore, a single landmark pair change influences the whole registration result, while if deformations are rather local a limited influence to some image parts is desired. Some methods were presented to circumvent this disadvantage, as, for instance, the use of radial basis functions with compact support [12], the weakening of the interpolation conditions [10], the introduction of a new class of elastic body splines [13], and the employment of the Lobachevsky splines [3]. However, it is well known in the literature that radial basis functions with compact support are less accurate than radial basis functions with global support, while considering approximation instead of interpolation, in particular when the number of points is small, does not always assure good results (see for instance [11]). On the other hand the class of elastic body splines is, as far as we know, under investigation, since the optimal choice of the parameter involved in the scheme requires further mathematical and experimental analysis (see [13], p. 274).

In this paper we propose the employment of a modified Shepard method, which uses radial basis functions as nodal functions (a first sketch of the technique was presented in [8]); this modification gives rise to a local interpolation method. Shepard method is one of the most commonly used techniques for scattered data interpolation, also known in literature as *Inverse Distance Weighted* or *Cardinal Radial Basis* interpolation methods (see, for instance, [2, 4, 23] and references therein). The local scheme is well known in approximation theory (see, for example, [4, 14]), but, as far as we know, never used in the image registration context. Moreover, this approach can be applied for the registration of $2D$ and $3D$ tomographic images (MR, CT).

The paper is organized as follows. In section 2 some preliminary definitions and the mathematical formulation of the landmark-based registration problem are given. We briefly recall radial basis function transformations in section 3, and in section 4 thin plate spline transformations. Section 5 is devoted to formulate the local radial basis function transformation technique, giving the corresponding transformation algorithm in section 6. Finally, section 7 contains some numerical results obtained for some test cases, and section 8 the concluding remarks and future work.

2 Landmark-Based Registration Problem

Let $S = \{\mathbf{x}_i^S, i = 1, \dots, n\}$ and $T = \{\mathbf{x}_i^T, i = 1, \dots, n\}$ be two sets each containing n point-landmarks in the source image and in the target image, respectively. The registration problem reads as follows.

Problem 1. Find a continuous transformation $\mathbf{h} : \mathbb{R}^d \to \mathbb{R}^d$ within a suitable Hilbert space $\mathcal{H}$ of admissible functions, such that

$$\mathbf{h}(\mathbf{x}_i^S) = \mathbf{x}_i^T, \qquad i = 1, \dots, n. \tag{1}$$

Each coordinate of the transformation function is often calculated separately, i.e. the interpolation problem $h_k : \mathbb{R}^d \to \mathbb{R}$ is solved for each coordinate $k = 1, \dots, d$, with the corresponding conditions $h_k(\mathbf{x}_i^S) = \mathbf{x}_{i,k}^T$, $i = 1, \dots, n$.

We give also some preliminary definitions, following [15].

Definition 1. An image transformation is called *rigid* when only translations and rotations are allowed. If the transformation maps parallel lines onto parallel lines, it is called *affine*. If it maps lines onto lines, it is called *projective*. Finally, if it maps lines onto curves, it is called *elastic*.

Definition 2. An image transfomation is called *global* if it applies to the entire image, and *local* if each subsection of the image has its own transformation defined.

In this paper we will consider a local transformation method for elastic image registration.

3 Radial Basis Function Transformations

Applying a radial basis function approach, the general coordinate of the transformation function $h_k(\mathbf{x})$, $k = 1, \dots d$, (in the following, we write for simplicity $h(\mathbf{x})$ instead of $h_k(\mathbf{x})$) is assumed to have the form

$$h(\mathbf{x}) = \varphi(\mathbf{x}) + p(\mathbf{x}), \tag{2}$$

where φ is a radial basis function spanning an n-dimensional space of functions depending only on the source landmarks $\mathbf{x}_i^S$, and $p \in \mathcal{P}_{m-1}^d \equiv \mathcal{P}_{m-1}(\mathbb{R}^d)$, i.e. p is a sum of polynomials up to degree $m-1$. The space $\mathcal{P}_{m-1}^d = \text{span}\{\pi_k\}_{k=1}^M$ has dimension $M = (d+m-1)!/(d!(m-1)!)$, which must be lower than n. This condition determines the minimum number of landmarks. We can rewrite (2) in the extended form

$$h(\mathbf{x}) = \sum_{i=1}^{n} c_i \Phi(||\mathbf{x} - \mathbf{x}_i^S||) + \sum_{j=1}^{M} a_j \pi_j(\mathbf{x}), \tag{3}$$

where $||\mathbf{x} - \mathbf{x}_i^S|| = ||\mathbf{r}||$ is the Euclidean distance from $\mathbf{x}$ to $\mathbf{x}_i^S$, $\Phi(r) = \Phi(||\mathbf{r}||)$, a function depending only on the distance, and c_i and a_j are coefficients.

To compute the coefficients $\mathbf{a} = (a_1, \dots, a_M)^T$ and $\mathbf{c} = (c_1, \dots, c_n)^T$ in (3), the following system of linear equations needs to be solved:

$$\begin{array}{rcl} \mathbf{Kc} + \mathbf{Pa} & = & \mathbf{v} \\ \mathbf{P}^T\mathbf{c} & = & \mathbf{0}, \end{array} \tag{4}$$

where $\mathbf{K} = \{\Phi(||\mathbf{x}_j^S - \mathbf{x}_i^S||)\}$ is a $n \times n$ matrix, $\mathbf{P} = \{\pi_j(\mathbf{x}_i^S)\}$ is a $n \times M$ matrix, and $\mathbf{v}$ denotes the column vector of the k-th coordinate of the target points $\mathbf{x}_i^T$. It is obtained by requiring that h satisfies the interpolation conditions and the side conditions $\sum_{i=1}^n c_i \pi_j(\mathbf{x}_i^S) = 0$, for $j = 1, \dots, M$. The equation $\mathbf{P}^T\mathbf{c} = \mathbf{0}$ represents the boundary conditions.

The most popular choices for Φ are given in Table 1.

Among them, thin plate spline, Gaussians and multiquadrics are very suitable for image registration. To solve for the coefficients a_j and c_i in (4) for all possible sets of landmarks, it is required that the linear system be non-singular. The polynomial part of h is necessary to guarantee the non-singularity when Φ is the thin plate spline or the multiquadric. The matrix of the linear system is in general dense, since the functions do not have compact support, and are ill-conditioned. This happens also in image registration applications, even if the RBF transformations work only on a relatively small number of points to be interpolated.

Radial Basis Function	Expression
Linear	r
Gaussians	$\mathrm{e}^{-\beta r^2}, \ \beta > 0$
Thin plate spline	$r^{2m-d} \log r, \ 2m-d \in 2\mathbb{N}$
Multiquadrics	$(r^2+\gamma^2)^{1/2}, \ \gamma > 0$
Inverse Multiquadrics	$(r^2+\gamma^2)^{-1/2}, \ \gamma > 0$

Table 1: Radial basis functions $\Phi(r)$.

4 Thin Plate Spline Transformations

The thin plate spline interpolation problem consists in finding a continuous transformation $\mathbf{h} : \mathbb{R}^d \to \mathbb{R}^d$ within a suitable Hilbert space $\mathcal{H}$ of admissible functions, which minimizes a given functional $J : \mathcal{H} \to \mathbb{R}$ and satisfies the interpolation conditions (1).

The minimizing functional represents the bending energy of a thin plate separately for each component h_k, $k = 1, \ldots, d$, of the transformation $\mathbf{h}$. Thus, the functional $J(\mathbf{h})$ can be separated into a sum of similar functionals that only depend on one component h_k of $\mathbf{h}$, and the problem of finding $\mathbf{h}$ can be decomposed into d problems.

In the case of d-dimensional images and for an arbitrary order m of derivatives in the functional we have

$$J_m^d(\mathbf{h}) = \sum_{k=1}^{d} J_m^d(h_k),$$

where the single functionals read as

$$J_m^d(h) = \sum_{\alpha_1+\cdots+\alpha_d=m} \frac{m!}{\alpha_1! \cdots \alpha_d!} \int_{\mathbb{R}^d} \left(\frac{\partial^m h}{\partial x_1^{\alpha_1} \cdots \partial x_d^{\alpha_d}} \right)^2 d\mathbf{x} \tag{5}$$

with α_k being positive integers. The functional is invariant under affine transformations like scaling, rotation and translation. This property makes it particularly suitable to provide a quantitative measure of deformations.

The solution of minimizing the functional (5) can be written in the analytic form (3). In particular, if we take the space of functions on $\mathbb{R}^d$ for which all partial derivatives of total order m are square integrable (i.e. are in $L_2(\mathbb{R}^d)$) as Sobolev space, we obtain the kernel

$$\Phi(||\mathbf{x}-\mathbf{x}_i^S||) = \begin{cases} \theta_{m,d} \left|\left|\mathbf{x}-\mathbf{x}_i^S\right|\right|^{2m-d} \ln \left|\left|\mathbf{x}-\mathbf{x}_i^S\right|\right|, & 2m-d \in 2\mathbb{N}, \\ \theta_{m,d} \left|\left|\mathbf{x}-\mathbf{x}_i^S\right|\right|^{2m-d}, & \text{otherwise}, \end{cases}$$

with $\theta_{m,d}$ as defined in [22].

5 Local Radial Basis Function Transformations

In this section we describe a local transformation method for landmark–based registration. It consists of a local Shepard method, also known as *modified Shepard method* in the multivariate interpolation context (see e.g. [4, 14]). The approach we propose exploits the characteristic of the classical Shepard formula combined with local RBF interpolants and localizing functions. This special transformation scheme is a flexible and powerful mathematical tool for scattered data interpolation and allows to overcome some drawbacks due to the classical Shepard formula and RBF method, such as inaccuracy, unstability and global support.

Let us consider the following definition of the modified Shepard method formulated in the context of image registration.

Definition 3. Given a set of source landmark points $S = \{\mathbf{x}_i^S, i = 1, \dots, n\}$, arbitrarily distributed in a domain $D \subset \mathbb{R}^d$, with associated the corresponding set of target landmark points $T = \{\mathbf{x}_i^T, i = 1, \dots, n\}$ in D, a *modified Shepard transformation* $\mathbf{H} : \mathbb{R}^d \to \mathbb{R}^d$ is such that each component takes the form

$$H_k(\mathbf{x}) = \sum_{j=1}^{n} Q_j^k(\mathbf{x}) \bar{W}_j^k(\mathbf{x}), \qquad k = 1, \dots, d,$$

where the nodal functions $Q_j^k(\mathbf{x})$, $j = 1, \dots, n$, are local approximants in $\mathbf{x}_j^S$ relative to the subset

$$\mathcal{N}_j = \{\mathbf{x}_i^S \in S,\ i \in I_j\},$$

I_j being the set of indices of n_Q neighbours of $\mathbf{x}_j^S$, and $\bar{W}_j^k(\mathbf{x})$, $j = 1, \dots, n$, are the weight functions defined as follows

$$\bar{W}_j^k(\mathbf{x}) = \frac{W_j^k(\mathbf{x})}{\sum_{u=1}^{n} W_u^k(\mathbf{x})}, \quad j = 1, \dots, n,$$

with

$$W_j^k(\mathbf{x}) = \tau_j(||\mathbf{x} - \mathbf{x}_j^S||)/\alpha(||\mathbf{x} - \mathbf{x}_j^S||),$$

$\tau_j(||\mathbf{x} - \mathbf{x}_j^S||)$ being a nonnegative real localizing function with compact support, called the *step function*, and α the radial basis function $\alpha(||\mathbf{x} - \mathbf{x}_j^S||) = ||\mathbf{x} - \mathbf{x}_j^S||^2$, where $||\cdot||$ is the Euclidean distance. Note that the transformation $\mathbf{H}$ (or, equivalently, each component H_k, $k = 1, \dots, d$) is evaluated at $\mathbf{x}$ considering only a certain number of landmarks closest to $\mathbf{x}$. We denote by n_W this number of landmarks.

In the bivariate case, denoting by (u, v) a general point in $\mathbb{R}^2$, the simplest case of the step function is

$$\tau(||(u, v) - (u_i, v_i)||) = \begin{cases} 1 & (u_i, v_i) \in [u - \delta, u + \delta] \times [v - \epsilon, v + \epsilon], \\ 0 & \text{otherwise}, \end{cases}$$

depending on values of δ and ϵ, with $\delta, \epsilon > 0$. In general, it identifies a local rectangular (square, if $\delta = \epsilon$) neighborhood, but other possible choices are admissible or even better.

The influence of the approximant Q_j^k is then limited by a weight function which decreases with the inverse of the distance from $\mathbf{x}_j^S$. A suitable choice for the local approximants Q_j^k is given by radial basis functions.

6 Local Radial Basis Function Transformation Algorithm

The transformation algorithm can be briefly described as follows:

For each evaluation point $\mathbf{y} \in \mathcal{Y}$

`Step 1.` Construct a local neighborhood, whose size depends on the sample dimension n in the domain D.

`Step 2.` Search and order all the data points belonging to a neighborhood by a distance-based sorting procedure.

`Step 3.` Reduce the number of data points to be interpolated to n_W, for each neighborhood.

`Step 4.` Find a RBF interpolant, computed using n_Q points, taking into account only the closest points n_W to $\mathbf{y}$.

`Step 5.` Evaluate $\mathbf{H}(\mathbf{y})$ by applying the modified Shepard formula.

The choice of the local (square) neighborhood size is carried out automatically in relation to the sample dimension n. Supposing to have a uniform distribution of points throughout the domain D, each local neighborhood contains a prefixed number of points. The condition is satisfied, taking into account the sample dimension n; this allows us to introduce a rule, which connects the half-size δ of a square neighborhood and the dimension n, i.e. $\delta = w/\sqrt{n}$, where w is a suitably chosen real number. Note that the value of w expresses the density of points that are contained in each neighborhood.

7 Numerical Results

In this section we show the applicability of the local transformation algorithm, referring to examples in [12] and [13] which concern the registration of elastic images. With regard to rigid or affine registration techniques in which we have rigid objects embedded in elastic material changing their position or form, the approach we propose can cope with local differences between corresponding images. In general, these differences are caused by the physical deformation of human tissue due to surgeries or pathological processes such as tumor growth or tumor resection.

7.1 Test Case 1

These examples simulate typical medical cases, where image portions shift and either shrink or grow. The grids are transformed using 32 landmarks and, in the case of square shift, also 4 quasi–landmarks to prevent an overall shift. The source and target image landmarks, both shown in the left images in Fig. 1 and Fig. 2, are marked by a circle ($\circ$) and a star ($\star$), respectively. In these cases we obtain better results using Gaussian interpolants. The center images show the registration results using Gaussian with $\beta = 1$. The right images are obtained employing the local transformation algorithm with $n_Q = n_W = 10$, for the modified Shepard method, and $\beta = 1$ for the Gaussian.

7.2 Test Case 2

In the following, we consider two simple models for the expansion and the resection of a tumor in surrounding elastic brain tissue (see Fig. 3). In our models the outer circle corresponds to the skull bone, which is assumed to be rigid. The inner circle represents the boundary of the tumor, whereas the space between the inner and the outer circle is assumed to be filled with elastic material, which corresponds to brain tissue.

In these experiments we compare the registration results obtained by using the local Shepard method with TPSs as nodal functions, and the global TPS method.

The grids are transformed using 20 equidistant landmarks placed on the inner circle and, to prevent an overall shift, also 40 quasi–landmarks, i.e. landmarks at invariant positions, at the outer circle in the source and target images. These point–landmarks, both shown in the left images in Fig. 4 and Fig. 5, are marked by a circle ($\circ$) and a star ($\star$), respectively. The center images show the

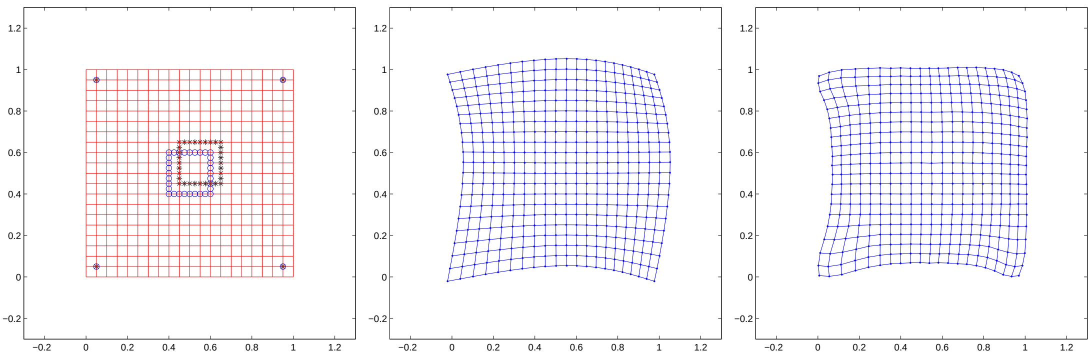

Figure 1: Shift of a square: 32 source and target landmarks and 4 quasi–landmarks (left), registration results using Gaussian (center) and local Gaussian–Shepard method (right).

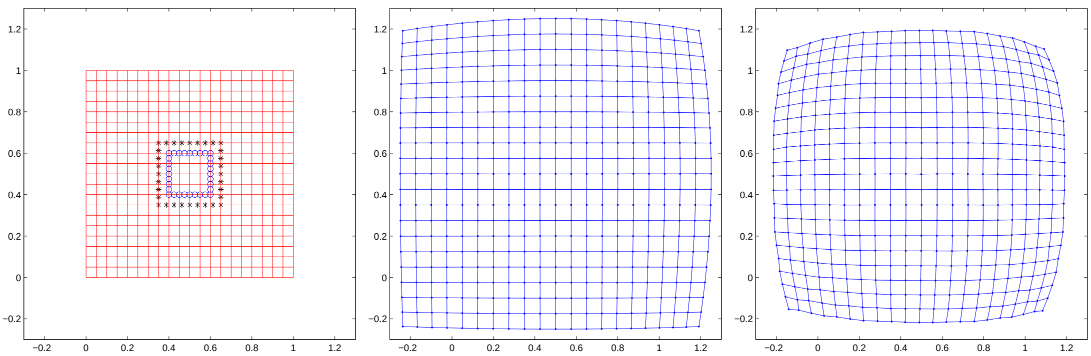

Figure 2: Scaling of a square: 32 source and target landmarks (left), registration results using Gaussian (center) and local Gaussian–Shepard method (right).

registration results using TPS. The right images are obtained employing the local transformation algorithm, that is, the modified Shepard method.

Quantitative graphics for the accuracy of the registration results are shown in Fig. 6 and Fig. 7. Here, we present the maximum absolute errors (MAEs) and the root mean squares errors (RMSEs), obtained by applying the local Shepard method, varying the parameters n_Q and n_W. These errors are found computing the distances between the displacements of grid points $\mathbf{y} \in \mathcal{Y}$ and the values of the modified Shepard formula $\mathbf{H}(\mathbf{y})$. They assume the following form

$$\mathrm{MAE} = \max_{\mathbf{y} \in \mathcal{Y}} \|\mathbf{y} - \mathbf{H}(\mathbf{y})\|,$$

$$\mathrm{RMSE} = \sqrt{\frac{\sum_{\mathbf{y} \in \mathcal{Y}} \|\mathbf{y} - \mathbf{H}(\mathbf{y})\|^2}{\sum_{\mathbf{y} \in \mathcal{Y}} 1}},$$

where $\|\cdot\|$ is the Euclidean norm.

Thus, exploiting the analysis of errors in Fig. 6 and Fig. 7, we can take "optimal" values for n_Q and n_W and compare the registration results, obtained by applying global and local RBF approaches. Their comparison points out the goodness and the effectiveness of our local method.

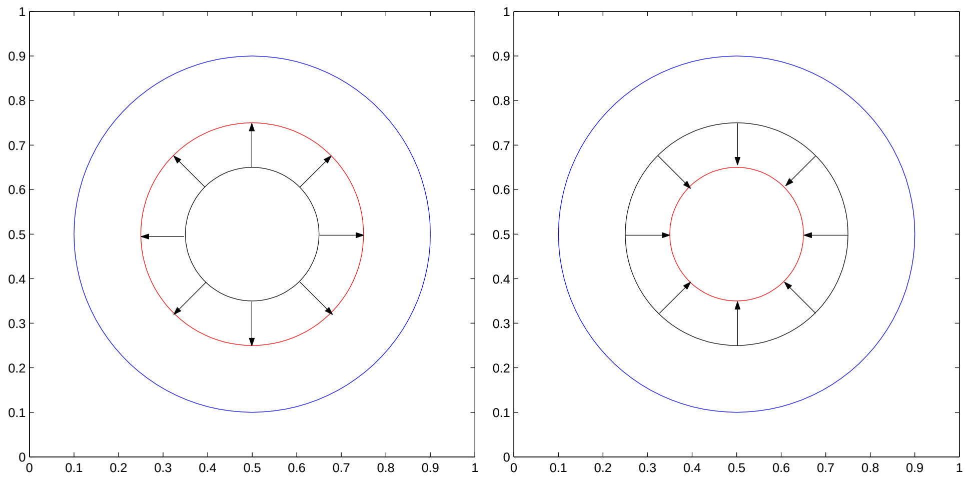

Figure 3: Models of an expanding tumor (left) and a tumor resection (right).

In the tumor expansion model, considering $n_Q = 3$ and $n_W = 6$ for the modified Shepard method, we have a MAE $= 1.2936\text{E}-1$ and a RMSE $= 5.1378\text{E}-2$, whereas the global method produces a MAE $= 1.2485\text{E}-1$ and a RMSE $= 6.2301\text{E}-2$. Conversely, in the tumor resection model the local method (with $n_Q = 6$ and $n_W = 9$) yields a MAE $= 1.0159\text{E}-1$ and a RMSE $= 4.3550\text{E}-2$, while the global one gives a MAE $= 1.7681\text{E}-1$ and a RMSE $= 7.9885\text{E}-2$.

8 Concluding Remarks and Future Work

We presented a local transformation method and the relative algorithm for landmark-based registration of medical images. It is based on a local interpolation method, which is a mathematical tool well known in approximation theory but, as far as we know, never used in this context.

Numerical results show its efficiency in some test cases: root mean square and maximum absolute errors are comparable and often better than those obtained with the global approach. Moreover, in the transformed images the deformations are limited. The registration results we obtained point out that the local transformation technique compares well with the global one, and in some cases it is superior. In particular, the former is preferable when the number of landmarks is large, since its main features are the locality and the stability. The drawback of this technique is the need of a manual determination of the local parameters n_Q and n_W. An automatic choice would be desirable and is currently under investigation. However an appropriate selection of the optimal values for the localization parameters n_Q and n_W, justified by extensive experimental tests, should be made taking $n_Q = 10$, $n_W = 10$, when the landmarks are situated in a small portion of the image, and in the ranges $n_Q = 3 \div 6$, $n_W = 6 \div 9$, when the landmarks are on a large portion of the image.

Furthermore, we are also performing numerical experiments concerning the registration of 2D tomographic images.

Acknowledgment

The authors thank the anonymous referees for their helpful and constructive comments.

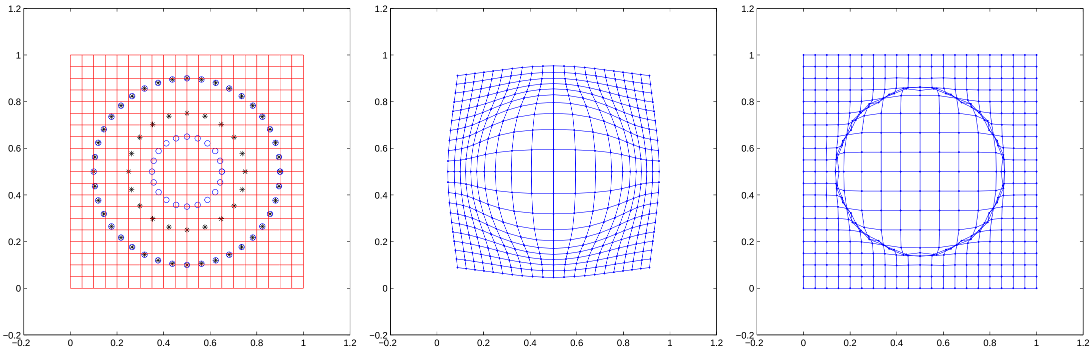

Figure 4: Expansion of a tumor: 20 source and target landmarks and 40 quasi–landmarks (left), registration results obtained by using global TPS (center) and local TPS–Shepard method with $n_Q = 6$ and $n_W = 9$ (right).

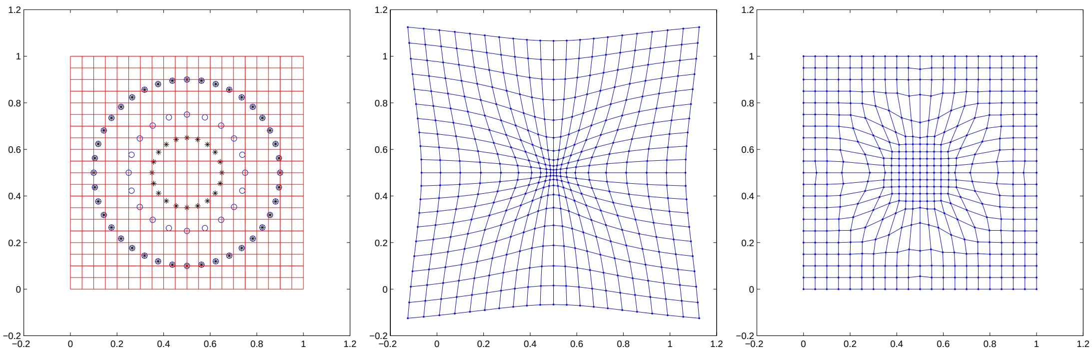

Figure 5: Resection of a tumor: 20 source and target landmarks and 40 quasi–landmarks (left), registration results obtained by using global TPS (center) and local TPS–Shepard method with $n_Q = 3$ and $n_W = 6$ (right).

The work described in this paper is partially supported by the Austrian GRID project, funded by the Austrian BMBWK (Federal Ministry for Education, Science and Culture) under contract GZ 4003/2-VI/4c/2004./. The first two authors gratefully acknowledge the support of Department of Mathematics, University of Turin, project "Modelli Matematici Avanzati per le Applicazioni e il Calcolo Scientifico – 2005".

References

[1] H. Akkari, I. Bhouri, P. Dubois, and M.H. Bedoui, On the relations between 2D and 3D fractal dimensions: theoretical approach and clinical application in bone imaging, *Math. Model. Nat. Phenom.* **3** (2008), 48–75.

[2] G. Allasia, Cardinal basis interpolation on multivariate scattered data, *Nonlinear Anal. Forum* **6** (2001), 1–13.

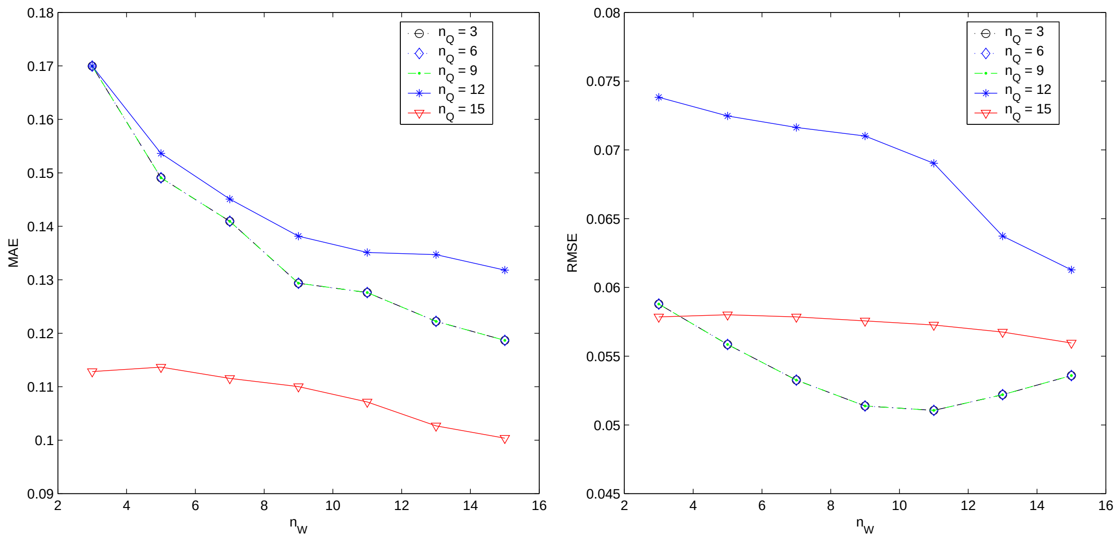

Figure 6: Tumor expansion: MAEs and RMSEs obtained by applying the local Shepard method, varying the parameters n_Q and n_W.

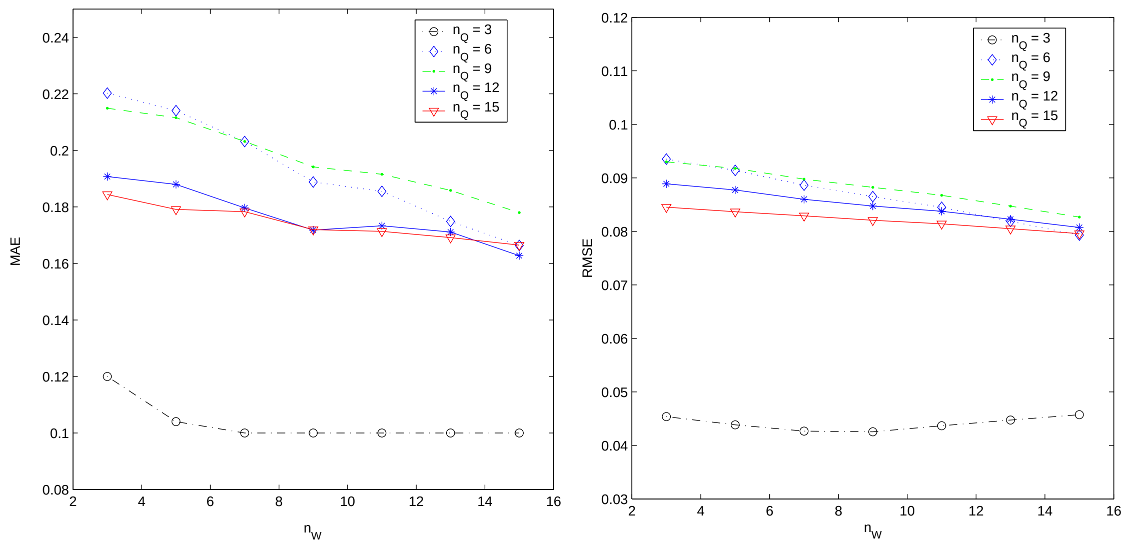

Figure 7: Tumor resection: MAEs and RMSEs obtained by applying the local Shepard method, varying the parameters n_Q and n_W.

[3] G. Allasia, R. Cavoretto, A. De Rossi, B. Quatember, W. Recheis, M. Mayr, and S. Demertzis, Radial basis functions and splines for landmark-based registration of medical images, in Proceedings of the International Conference on Numerical Analysis and Applied Mathematics 2010 (ICNAAM 10), AIP Conference Proceedings, T.E. Simos, G. Psihoyios, C. Tsitouras (eds.), vol. 1281, Melville, New York, 2010, 716–719.

[4] G. Allasia, R. Besenghi, R. Cavoretto, and A. De Rossi, Scattered and track data interpolation using an efficient strip searching procedure, *Appl. Math. Comput.* **217** (2011), 5949–5966.

[5] A.P. Benson, S.H. Gilbert, P. Li, S.M. Newton, and A.V. Holden, Reconstruction and quantification of diffusion tensor imaging-derived cardiac fibre and sheet structure in ventricular regions used in studies of excitation propagation, *Math. Model. Nat. Phenom.* **3** (2008), 101–130.

[6] F. Bookstein, Principal warps: thin-plate splines and the decomposition of deformations, *IEEE Trans. Pattern Anal. Mach. Intell.* **11** (1989), 567–585.

[7] M.D. Buhmann, *Radial Basis Functions: Theory and Implementations*, Cambridge Monogr. Appl. Comput. Math., vol. 12, Cambridge Univ. Press, Cambridge, 2003.

[8] R. Cavoretto, and A. De Rossi, A local IDW transformation algorithm for medical image registration, in Proceedings of the International Conference on Numerical Analysis and Applied Mathematics 2008 (ICNAAM 08), AIP Conference Proceedings, T.E. Simos, G. Psihoyios, Ch. Tsitouras (eds.), vol. 1048, Melville, New York, 2008, 970–973.

[9] M.S. De Craene, B. Macq, F. Marques, P. Salembier, and S.K. Warfield, Unbiased group-wise alignment by iterative central tendency estimations, *Math. Model. Nat. Phenom* **3** (2008), 2–32.

[10] G. Donato, and S. Belongie, Approximate thin plate spline mappings, Computer Vision-ECCV'2002: 7th European Conference on Computer Vision, Copenhagen, Denmark, May 28-31, 2002, 21–31.

[11] G.E. Fasshauer, *Meshfree Approximation Methods with MATLAB*, World Scientific Publishers, Singapore, 2007.

[12] M. Fornefett, K. Rohr, and H.S. Stiehl, Radial basis functions with compact support for elastic registration of medical images, *Image and Vision Computing* **19** (2001), 87–96.

[13] J. Kohlrausch, K. Rohr, and H.S. Stiehl, A new class of elastic body splines for nonrigid registration of medical images, *J. Math. Imaging Vision* **23** (2005), 253–280.

[14] D. Lazzaro, and L.B. Montefusco, Radial basis functions for the multivariate interpolation of large scattered data sets, *J. Comput. Appl. Math.* **140** (2002), 521–536.

[15] J.B.A. Maintz, and M.A. Viergever, A survey of medical image registration, *Medical Image Analysis* **2** (1998), 1–37.

[16] Medical Image Processing, Analysis and Visualization (MIPAV), http://mipav.cit.nih.gov, software package.

[17] J. Modersitzki, *Numerical Methods for Image Registration*, Oxford Univ. Press, Oxford, 2004.

[18] J. Modersitzki, *FAIR: Flexible Algorithms for Image Registration*, Fundamentals of Algorithms 6, SIAM, Philadelphia, PA, 2009.

[19] B. Quatember, M. Mayr, W. Recheis, S. Demertzis, G. Allasia, A. De Rossi, R. Cavoretto, and E. Venturino, Geometric modelling and motion analysis of the epicardial surface of the heart, *Math. Comput. Simulation* **81** (2010), 608–622.

[20] K. Rohr, *Landmark-Based Image Analysis, Using Geometric and Intensity Models*, Kluwer Academic Publishers, Norwell, MA, 2001.

[21] K. Rohr, Spline-based elastic image registration, *Proc. Appl. Math. Mech.* **3** (2003), 36–39.

[22] G. Wahba, *Spline Models for Observational Data*, Society for Industrial and Applied Mathematics, Philadelphia, Pennsylvania, 1990.

[23] H. Wendland, *Scattered Data Approximation*, Cambridge Monogr. Appl. Comput. Math., vol. 17, Cambridge Univ. Press, Cambridge, 2005.